JOURNAL OF TISSUE ENGINEERING AND REGENERATIVE MEDICINE
J Tissue Eng Regen Med 2010; **4**: 12–24.
Published online 15 October 2009 in Wiley InterScience (www.interscience.wiley.com) **DOI:** 10.1002/term.197

RESEARCH ARTICLE

Human tissue-engineered bone produced in clinically relevant amounts using a semi-automated perfusion bioreactor system: a preliminary study

F. W. Janssen[1,2]*, R. van Dijkhuizen-Radersma[2], A. Van Oorschot[3], J. Oostra[4], J. D. de Bruijn[2,5] and C. A. Van Blitterswijk[1]

[1]*Institute for Biomedical Technology, University of Twente, 3720 AB Bilthoven, The Netherlands*
[2]*Xpand Biotechnology BV, 3723 MB Bilthoven, The Netherlands*
[3]*IsoTis SA, 3723 MB, Bilthoven, The Netherlands*
[4]*Applikon Dependable Instruments B.V, 3100 AC Schiedam, The Netherlands*
[5]*Queen Mary University of London, UK*

Abstract

The aim of this study was to evaluate a semi-automated perfusion bioreactor system for the production of clinically relevant amounts of human tissue-engineered bone. Human bone marrow stromal cells (hBMSCs) of eight donors were dynamically seeded and proliferated in a perfusion bioreactor system in clinically relevant volumes (10 cm^3) of macroporous biphasic calcium phosphate scaffolds (BCP particles, 2–6 mm). Cell load and distribution were shown using methylene blue staining. MTT staining was used to demonstrate viability of the present cells. After 20 days of cultivation, the particles were covered with a homogeneous layer of viable cells. Online oxygen measurements confirmed the proliferation of hBMSCs in the bioreactor. After 20 days of cultivation, the hybrid constructs became interconnected and a dense layer of extracellular matrix was present, as visualized by scanning electron microscopy (SEM). Furthermore, the hBMSCs showed differentiation towards the osteogenic lineage as was indicated by collagen type I production and alkaline phosphatase (ALP) expression. We observed no significant differences in osteogenic gene expression profiles between static and dynamic conditions like ALP, BMP2, Id1, Id2, Smad6, collagen type I, osteocalcin, osteonectin and S100A4. For the donors that showed bone formation, dynamically cultured hybrid constructs showed the same amount of bone as the statically cultured hybrid constructs. Based on these results, we conclude that a semi-automated perfusion bioreactor system is capable of producing clinically relevant and viable amounts of human tissue-engineered bone that exhibit bone-forming potential after implantation in nude mice. **Copyright © 2009 John Wiley & Sons, Ltd.**

Received 3 July 2008; Revised 12 April 2009; Accepted 1 July 2009

Keywords **bioreactor; tissue engineering; bone; human bone marrow stem cells; perfusion; online measurement; *in vivo***

1. Introduction

Bone marrow stromal cells (BMSCs) have been extensively investigated in both experimental and clinical settings. These cells exhibit multipotency [1–3], which potentially enables them to be used for the treatment of several diseases [4,5]. In the field of tissue engineering, BMSCs have been used for bone repair, since one of their most important differentiation pathways seems to be osteogenic [6]. The proof of concept for bone tissue engineering by combining bone marrow stem cells with suitable biomaterials (hybrid constructs) has been shown both ectopically [7,8,12] and orthotopically in rodent studies [9–12].

*Correspondence to: F. W. Janssen, Institute for Biomedical Technology, University of Twente, Professor Bronkhorstlaan 10-D, PO Box 98, 3720 AB Bilthoven, The Netherlands.
E-mail: f.w.janssen@tnw.utwente.nl

Copyright © 2009 John Wiley & Sons, Ltd.

Although cell-based bone tissue engineering is a promising concept, there are still some problems which have to be solved in order to be clinically applicable [13]. First, osteogenic constructs are often produced by isolating osteoprogenitor cells from a marrow aspirate which are multiplied in tissue culture flasks and subsequently seeded on and in a three-dimensional (3D) scaffold [14,15]. It has been reported that the average amount of adult stem cells that can be differentiated into the osteogenic lineage from a patient is only about 1–10 per 100 000 cells present in the bone marrow [16], while 200–800 million adult stem cells are required for clinical use to repair a large bone defect [17]. Taking into account that an average bone marrow aspirate of 10 ml will harvest 500–8000 adult stem cells, up to a million-fold multiplication is needed for clinical treatment. For large-scale production, the current two-dimensional (2D) multiplication process in tissue culture flasks has some serious drawbacks. The flasks are limited in their productivity by the number of cells that can be supported by a given area, while repeated handling for culture maintenance makes the process labour-intensive and susceptible to contamination. Moreover, the microenvironment of the cells is not monitored and controlled, which results in suboptimal culture conditions [18]. Furthermore, the 2D proliferation of these cells is not comparable with the *in vivo* situation. It has been shown that 2D expanded BMSCs have a diminished differentiation capacity in comparison with those found in fresh bone marrow [19,20]. It is hypothesized that a 3D culture system may represent a physiologically more favourable environment for BMSCs than a tissue culture flask, as shown for several cell types [21].

Another challenge that complicates the clinical application of BMSCs in bone tissue engineering is the available amount of tissue-engineered product. Clinically useful volumes of hybrid constructs for spinal surgery vary in the range 4–15 cm^3 [22], whereas these amounts are often >20 cm^3 for some other orthopaedic applications [23]. Production of these amounts of hybrid construct is complicated because of potential mass transfer limitations with respect to the supply of oxygen and medium components. It is well known that mass transfer limitations occur during *in vitro* culture of various 3D constructs, resulting in a limited amount of cell growth into the 3D construct [24,25]. Bioreactors that perfuse medium through scaffolds allow the reduction of internal mass-transfer limitations and the exertion of mechanical forces by fluid flow [26]. Cultivation of osteoblast-like cells and rat bone marrow stem cells on 3D constructs in perfusion bioreactors have been shown to enhance growth, differentiation and mineralized matrix production *in vitro* [27–30]. Only few studies have shown *in vivo* bone formation of animal-derived hybrid constructs cultivated in perfusion bioreactors [31,32]. None of these studies were performed using human BMSCs. Previously, we have reported a direct perfusion bioreactor system that can drastically reduce the amount of space and handling steps involved and increase the volume of tissue-engineered product for bone tissue engineering. Furthermore, this system allowed the online monitoring of oxygen consumption during seeding and cultivation of the hybrid constructs [33]. We demonstrated that the produced hybrid constructs (using goat BMSCs as a model system) gave rise to *in vivo* bone formation after implantation in nude mice [32], whereas the bare scaffold showed no osteoinductive potential in nude mice [34]. In this study we evaluated the direct perfusion system for human bone tissue engineering. We report the cultivation of human BMSCs (hBMSCs) from eight different donors in 13 independent bioreactor runs. The runs varied in seeding density, perfusion rate and cultivation time. The obtained hybrid constructs were evaluated with respect to cell load, viability, *in vitro* differentiation and *in vivo* bone formation.

2. Materials and methods

2.1. Production of human hybrid constructs

2.1.1. Initial cell culturing of hBMSCs in tissue culture flasks

Human bone marrow aspirates were obtained from eight patients who had given written informed consent. The aspirates were isolated from the iliac crest and cultured as previously described in detail [20]. Culture medium comprised of α-MEM supplemented with 10% FBS, antibiotics, 0.1 mM L-ascorbic acid-2-phosphate, 2 mM L-glutamine, 1×10^5 mM dexamethasone and 1 ng/ml basic fibroblast growth factor (bFGF). hBMSCs were cultured at 37 °C in a humid atmosphere with 5% CO_2. At the end of the first passage (P1), the cells were cryopreserved. Within 12 months, the cryopreserved cells were thawed and replated in tissue culture flasks. When the cells were near confluence, they were washed with phosphate-buffered saline (PBS), enzymatically released by means of a 0.25% trypsin–EDTA solution and replated at a density of 5000 cells/cm^2. Subsequent passages were performed when cells were near confluence, usually 4–5 days later.

2.1.2. Scaffolds

Biphasic calcium phosphate scaffolds (BCP, OsSatura™, IsoTis, The Netherlands) were made of 36% macroporous (pores >100 μm) biphasic calcium phosphate. The total porosity of these scaffolds was 59% (average interconnected pore size = 388 μm of all the pores >100 μm) as measured by Hg porosity measurement. BCP scaffolds were produced according to the H_2O_2 method including naphthalene, as described previously [34]. The material was sintered at 1200 °C. The ceramic consisted of 80 ± 5% hydroxyapatite (HA) and 20 ± 5% tricalcium phosphate (TCP), as confirmed by X-ray diffraction and Fourier-transformed infrared spectroscopy (FITR), no additional impurities were detected. Granules of diameter 2–6 mm were γ-irradiated at a minimal dose of 25 kGy. 10 cm^3 of scaffold material consisted of 230 scaffolds

Copyright © 2009 John Wiley & Sons, Ltd.

DOI: 10.1002/term

±10%. The packed scaffold bed inside the bioreactor was visualized by microCT imaging and is depicted in Figure 1. Compaction density of the randomly stacked scaffold bed was 0.81 ± 0.02 as determined for five different 10 cm^3 batches.

2.1.3. The semi-automated bioreactor and bioreactor system

A direct perfusion flow bioreactor was used as described previously [32,33] and is schematically shown in Figure 2. In short, the bioreactor consists of an inner and outer housing, which were configured as coaxially disposed, nested cylinders. The bioreactor system comprised a bioreactor, a sterile fluid pathway (made of γ-sterilized PVC tubing, which had low gas permeability) that includes a medium supply vessel, a pump, an oxygenator and a waste vessel. The individual components of the bioreactor system can be detached in a sterile way by using a tube sealer (Teruseal™, Terumo). After sampling, these components can be attached again in a sterile way using a tube welder (TSCD™, Terumo). The fluid pathway contained a temperature sensor and two dissolved oxygen sensors, which were placed at the medium inlet and outlet of the bioreactor.

The entire bioreactor system was placed in a temperature-controlled box (incubation unit), which was kept at 37 °C. These incubation units lack a gas-controlled atmosphere and to supply the cells with oxygen and carbon dioxide, an oxygenator was developed. The oxygenator comprised a closed chamber containing a gas-permeable silicon tube. The gas environment in the chamber was kept at a constant level of 20% O_2 and 5% CO_2 and medium was pumped through the gas-permeable tube. This system enables a medium flow through the bioreactor of a constant pH and a constant oxygen concentration.

2.1.4. Seeding and culturing of hBMSCs in the bioreactor system

hBMSCs, cultured as described before, were suspended in culture medium and transported into a seeding vessel which was attached to the seeding loop of the bioreactor

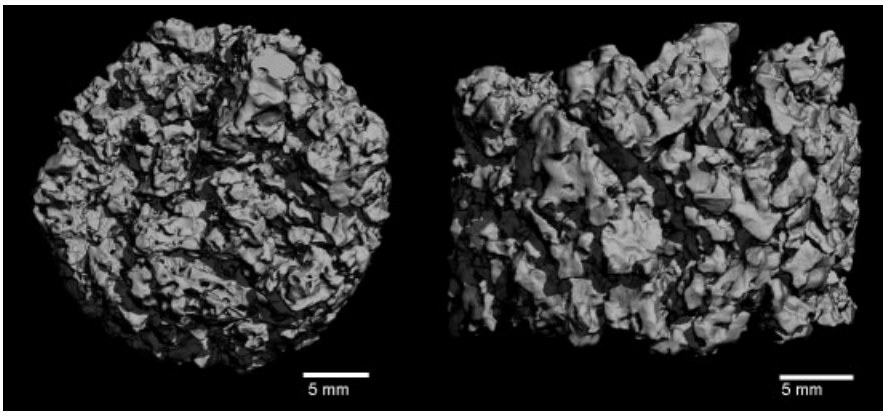

Figure 1. Micro CT images of the packed scaffold bed inside the bioreactor. View from the top (left) and the side (right)

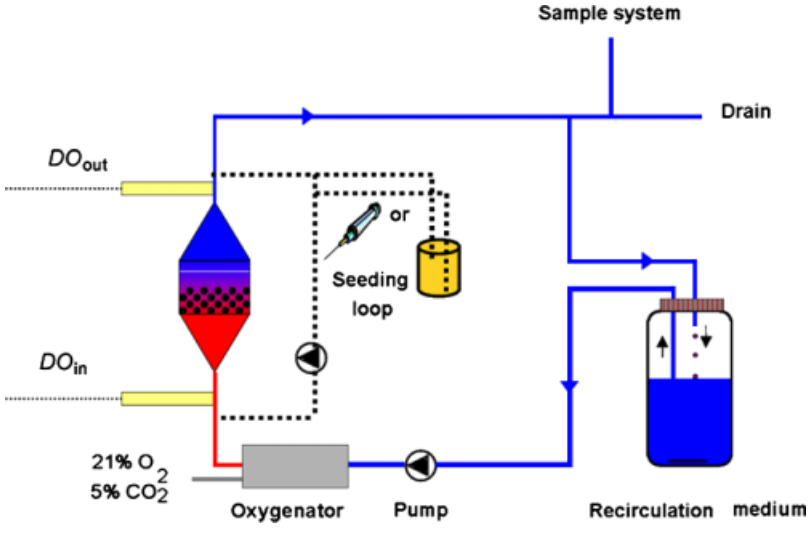

Figure 2. Process scheme bioreactor system. Medium is perfused from the bottom to the top, allowing a medium flow over and through the scaffold bed (stacked black dots). Two loops can be distinguished: a seeding loop (dashed line) and a proliferation loop (solid line)

Copyright © 2009 John Wiley & Sons, Ltd.

DOI: 10.1002/term

system described in Figure 2. Before cell seeding, 10 cm^3 scaffold material in the bioreactor (dimensions of the bioreactor chamber: diameter, 2.8 cm; height, 2.6 cm) was flushed with cultivation medium in order to pre-wet the particles and allow serum proteins to attach to the scaffold surface. hBMSCs of various passages and in different concentrations were suspended in 20 ml cultivation medium and seeded on 10 cm^3 scaffold material in a bioreactor system. hBMSCs of eight different human donors were used in a total of 13 separate bioreactor runs. An overview of all the experiments executed is depicted in Table 1.

Cell seeding took place by closing the recirculation loop and circulating the cell suspension through the seeding loop for 4 h at 4 ml/min (108 μm/s, unless stated otherwise), flow direction from bottom to top. After seeding, the seeding loop was closed and fresh medium was flushed through the bioreactor and tubing into the waste vessel (connected to the drain) to remove any non-adhered cells. After the flush period, the fluid path towards the drain was closed and, unless stated otherwise, medium recirculation was started at 4 ml/min (108 μm/s), in order to promote proliferation of the attached hBMSCs. The culture medium (with a composition as described before) in the recirculation loop was refreshed twice every week. During cultivation at 37 °C, three to five scaffold samples were taken from three different positions of the bioreactor (top, middle and bottom sections) at several time points. These samples were used for Methylene Blue (MB) and MTT staining. At the end of the cultivation period, random scaffold samples were taken for quantitative PCR (run Nos 11–13) and implantation studies in nude mice (all runs).

2.1.5. Static seeding and culturing

Static control scaffolds (48 particles, approximately 2 cm^3) were statically seeded with hBMSCs placed in a 25-well bacteriological-grade plate. Particles were placed in groups of three particles and 100 μl of a cell suspension (with a cell density comparable to the dynamic cell suspension) was applied on top of the particles. Cells were allowed to attach for 4 h at 37 °C, after which an additional 2 ml culture medium was added to each well. Cells were statically cultured at 37 °C in a humid atmosphere with 5% CO_2 and the cultivation medium was changed twice every week. Culture times of the static hybrid constructs were identical to the dynamically cultured constructs (see Table 1).

Table 1. Schematic overview of the bioreactor runs and process conditions

Run No.	Donor No.	Gender/age	Passage No.	Amounts of hBMSCs seeded ($\times 10^6$)	Cultivation time (days)
1	1	M/72	2	1	20
2	1		2	6	20
3	1		2	12	20
4	2	M/44	2	12	20
5	3	F/62	1	1	20
6	3		1	1	20
7	4	M/75	1	1	20
8	4		1	4	20
9	5	F/24	5	12	40
10*	5		2	12	7
11*	6	M/63	2	12	7
12*	7	F/68	2	12	7
13*	8	M/21	2	12	7

*Hybrid constructs in runs 10–13 were seeded statically.

2.1.6. Online oxygen measurement

The oxygen concentration was measured online in the medium inlet and medium outlet during dynamic proliferation, as can be seen in the process scheme in Figure 2. The oxygen electrodes used were sterilizable dissolved oxygen sensors from Applisens (Applikon, The Netherlands). In previous studies we showed that the difference in oxygen concentration between the medium inlet and medium outlet (ΔDO), when assuming a constant specific oxygen consumption (q_o), liquid volume of the bioreactor (V_l) and perfusion flow rate (F_l), is directly proportional to the biomass concentration [32,33].

2.1.7. Measurement of metabolites

Metabolites in the cultivation medium (glucose, lactate and ammonia) were measured in time using the Vitros DT 60 medium analyser. Dilutions for ammonia measurements were made in phosphate buffer, pH 7.5.

2.2. Characterization of human hybrid constructs

2.2.1. Cell distribution, load and viability

Cell distribution and cell load on the particles in the bioreactor were qualitatively assessed by using MB staining. After sampling, cells on the particles were fixed in 1.5% glutaraldehyde in 0.14 M cacodylic buffer, pH 7.4 ± 0.1 adjusted with 1 M HCl. After fixation, 1% methylene blue solution was added and incubated for 60 s and washed twice with PBS in order to remove non-bound methylene blue. Cells on the particles were visualized using light microscopy. For measuring cell viability, MTT staining was used. A solution of 1% MTT was applied on the particles containing cells. After 4 h of incubation, the MTT solution was removed by flushing the particles with PBS. Particles and cells were visualized using light microscopy.

2.2.2. Alkaline phosphatase staining

Expression of alkaline phosphatase (ALP) was evaluated by an Azo-dye method. Briefly, hybrid constructs were washed twice with PBS and fixed for 2 h in 4% paraformaldehyde. After washing the hybrid constructs twice with PBS, the samples were incubated in a naphthol

Copyright © 2009 John Wiley & Sons, Ltd.

DOI: 10.1002/term

AS-BI phosphate solution (6-bromo-2-phosphohydroxy-3-naphthoic acid *o*-anisidide) containing 0.1% w/w fast blue R salt (Sigma, The Netherlands) for 15 min at room temperature. Prior to incubation, the samples were incubated; the solution was filtered through a 0.2 µm filter in order to remove non-dissolved fast blue R salt.

2.2.3. Collagen type I assay

Expression of collagen type I by bone marrow stem cells cultured on particles was determined by immunohistochemistry. Fresh samples of hybrid constructs were hydrated by washing them in 100% PBS at 37 °C. PBS was removed and samples were blocked with 100% blocking buffer (BB, X0909, DAKO) for 60 min at room temperature. Dilutions of the primary antibody (mouse monoclonal to collagen type 1, reacts with human and goat, Abcam Ab23446, CSI 008-01) were made in PBS with 10% BB. Samples were incubated with the primary antibody at 4 °C for 16 h and subsequently washed three times with PBS with 10% BB. Samples were incubated with a secondary antibody (rabbit polyclonal to mouse IgG with a horseradish peroxidase conjugate; Abcam, ab6728) for 60 min at room temperature. Samples were washed three times with PBS. Subsequently a DAB chromogen solution was prepared by adding three drops of DAB solution (3,3′-diaminobenzidine chromogen solution, DAKO) in 1 ml DAB buffer (buffer solution, pH 7.5, DAKO). Samples were incubated in 100 µl DAB chromogen solution for 10 min at room temperature. Positive (goat bone) and negative (incubations without primary antibody and particles without cells) controls were also included in this experiment.

2.2.4. SEM and EDX analysis

After the *in vitro* cultivation period, matrix formation was examined by scanning electron microscopy (ESEM) and energy dispersive X-ray analysis (EDX). Samples from cell–scaffold constructs for ESEM analysis were fixed, dehydrated, gold-coated and examined in an environmental scanning electron microscope (ESEM; XL30, ESEM-FEG, Philips, The Netherlands). EDX analysis was used to identify the chemical composition of structures present on the particles.

2.2.5. RNA isolation and quantitative PCR

The effect of static and dynamic culture systems on expression of osteogenic marker genes was analysed by isolating RNA at the end of the culture period for bioreactor runs 11–13. The RNA was isolated using a Trizol RNA kit (Qiagen) and DNase treated with 10 U RNase-free DNase I (Gibco) at 37 °C for 30 min. DNAse was inactivated at 72 °C for 15 min. 2 µg RNA was used for first-strand cDNA synthesis, using Superscript II (Invitrogen) according to the manufacturer's protocol. 1 µl 100 × diluted cDNA was used for collagen type 1 (COL1) and 18s rRNA amplification and 1 µl undiluted cDNA was used for other genes. PCR was performed on a Light Cycler real-time PCR machine (Roche), using a SYBR green I master mix (Invitrogen). Data was analysed using Light Cycler software version 3.5.3, using the fit point method by setting the noise band to the exponential phase of the reaction to exclude background fluorescence. Expression of osteogenic marker genes are calculated relative to *18s* rRNA levels by the comparative ΔCT method [35] and statistical significance was found using Student's *t*-test ($p < 0.05$).

2.2.6. In vivo bone formation

Random scaffold samples from bioreactors were taken after the *in vitro* cultivation period in a sterile LAF cabinet and were soaked in α-MEM supplemented with 1% penicillin/streptomycin. Prior to implantation, the samples were washed in PBS. Control scaffold samples that were statically seeded and cultured with cells for the same period of time were also implanted. Nude male mice (Hsd-cpb : NMRI-nu, Harlan) were anaesthetized by isoflurane inhalation and subcutaneous pockets were made. The number of implanted dynamically cultured hybrid constructs, the number of mice used and a picture of the subcutaneous implantation are depicted in Figure 3.

The incisions were closed using a vicryl 5-0 suture. After 6 weeks the mice were sacrificed using CO_2 and samples were explanted, fixed in 1.5% glutaraldehyde (Merck) in 0.14 M cacodylic acid (Fluka) buffer, pH 7.3.

The fixed samples were dehydrated and embedded in methyl methacrylate (Sigma) for sectioning. Approximately 10 µm thick, undecalcified sections were processed on a histological diamond saw (Leica Microtome, Nussloch, Germany). The sections were stained with 0.3% basic fuchsin and 1% methylene blue, in order to visualize bone formation. Histomorphometry was performed

Run #	Cultivation time in vitro (days)	Number of cultured hybrid constructs implanted per mouse	Number of mice used	Total number of implanted cultured hybrid constructs
1-8	20	6	2	12
9	40	6	6	36
10-13	7	3	10	30

Figure 3. Number of implanted dynamically cultured hybrid constructs and the numbers of mice used. Subcutaneous implantation of hybrid constructs is visualized. The black circle depicts a pocket containing three separate hybrid constructs

Copyright © 2009 John Wiley & Sons, Ltd.

DOI: 10.1002/term

by scanning histological slides of stained sections of the whole hybrid constructs (run Nos 10–13). At least three sections (from three separate hybrid constructs) for all conditions per mouse were made. From these scans, the surface area of the whole scaffold (region of interest, ROI), surface area of the BCP ceramic (MAT) and the surface area of formed bone (BONE) is determined. The ratio of total amount of bone formed as a percentage of the available pore area (BIP) is determined according to equation 1:

$$\mathrm{BIP} = \mathrm{BONE}/(\mathrm{ROI\text{-}MAT}) \times 100\% \quad (1)$$

The obtained results were tested for statistical significance using a two-tailed Student's t-test ($p < 0.05$).

3. Results and discussion

3.1. Production of human hybrid constructs in a perfusion bioreactor system

Because of known patient variability with respect to proliferation and differentiation capacity of hBMSCs [20,40], we cultured cells on BCP particles in the perfusion bioreactor system of eight different donors in 13 separate runs. The runs varied in seeding density, perfusion rate and cultivation time (see Table 1).

3.1.1. Effect of seeding density on hBMSC growth

In bioreactor runs 1–3 and 7–8, cells were cultured in different seeding densities for two donors. In runs 1–3, cells were cultured in three seeding densities (donor 1), varying in the range 1–12 million cells. Samples were taken after 3, 10 and 17 days and stained with MB to visualize cell load and cell distribution (Figure 4).

Initially, more cells were visible on the particles for the highest seeding density (Figure 4G). Between individual particles, variations in cell load existed and cells were not distributed homogeneously over the scaffold surface at the first time points (Figure 4A, D, G). An increase in cell load per scaffold in time was observed during the proliferation phase for all seeding densities. After 17 days, the particles were largely covered with a homogeneous cell layer for all seeding densities. At this time point, no differences were seen between the top, middle and bottom fractions of the bioreactor. Furthermore, there was no visual difference in cell load between the different seeding densities (Figure 4C, F, I). We observed identical trends for different seeding densities in runs 7 and 8 (data not shown). The oxygen consumption supported the observed cell growth patterns (Figure 5). The ingoing and outgoing dissolved oxygen concentrations were measured during proliferation in all three bioreactor runs. During proliferation, the inlet oxygen concentration was kept at a constant level of 100% by saturation of the medium in the oxygenator and the outlet oxygen concentration decreased in time. The difference between the ingoing and outgoing oxygen concentration (ΔDO) for runs 1–3 is depicted in Figure 5.

The ΔDO increases during cultivation and plateau values of about 18% were reached for all seeding densities. This plateau value is reached after approximately 10, 13 and 19 days when seeding 12, 6 and 1 million cells, respectively. During cultivation, the cell load on the particles could be correlated with the difference in oxygen consumption, which was already demonstrated for goat

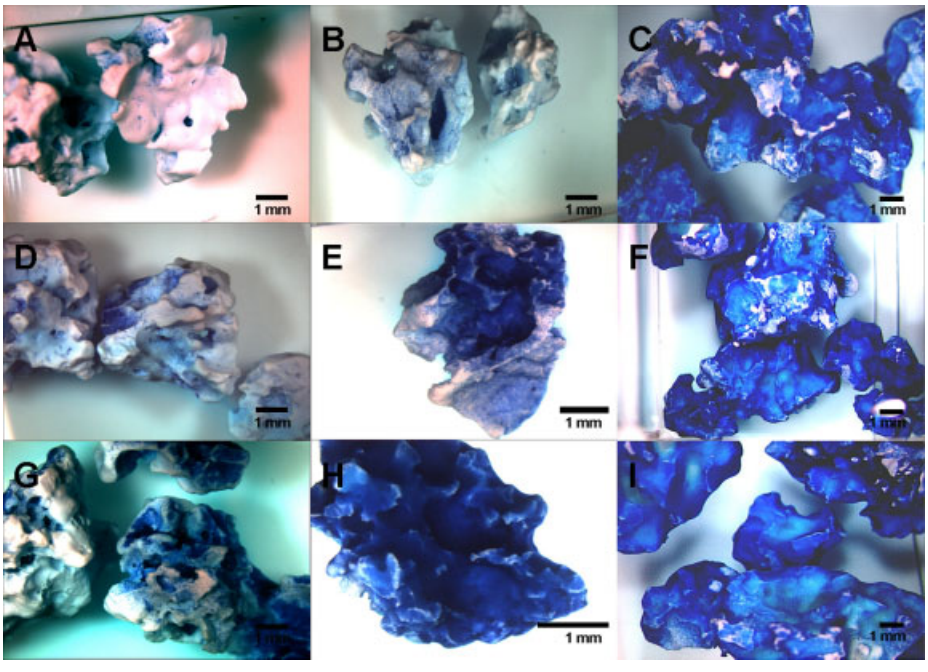

Figure 4. MB stained hBMSCs on OsSatura™ BCP particles after dynamic proliferation from left to right after 3, 10 and 17 days for three different seeding densities: 1 × 10^6 (A–C); 6 × 10^6 (D–F); and 12 × 10^6 (G–I)

Copyright © 2009 John Wiley & Sons, Ltd.

DOI: 10.1002/term

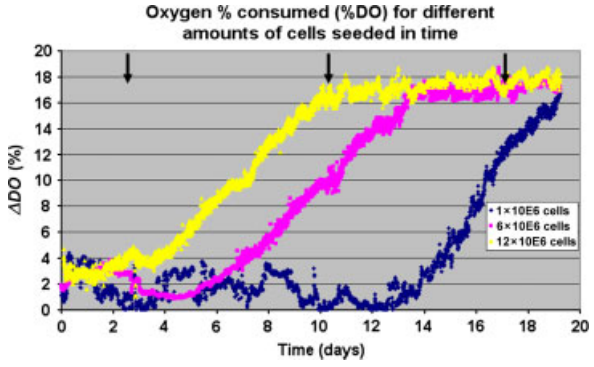

Figure 5. Net dissolved oxygen consumption ($\Delta DO = DO_{in} - DO_{out}$) during dynamic proliferation of hBMSCs from donor 1 on OsSatura™ BCP particles for three different seeding densities: 1 x 10^6; 6 x 10^6; and 12 10^6 cells. 100% indicates the concentration in cultivation medium, which is in equilibrium with the 20% oxygen in air. Arrows represent different time points (3, 10 and 17 days) for which the cell load is visualized by MB staining in Figure 4

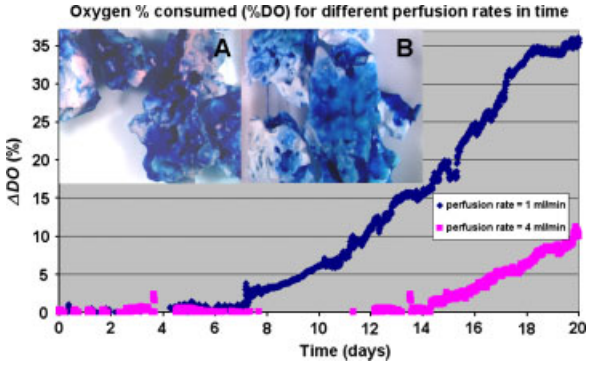

Figure 6. Net dissolved oxygen consumption ($\Delta DO = DO_{in} - DO_{out}$) during dynamic proliferation of hBMSCs from donor 3 on OsSatura™ BCP particles for two perfusion rates: 1 and 4 ml/min. (A) 1 ml/min and (B) 4 ml/min show MB-stained hBMSCs after 18 days of proliferation. 100% indicates the concentration in cultivation medium, which is in equilibrium with the 20% oxygen in air

BMSCs [31]. The arrows in Figure 5 correspond with the time points at which the cell loads are depicted in Figure 4. When the plateau values are reached (i.e. the ΔDO concentrations are equal for the three runs), the visually observed cell amounts present on the particles are identical. Furthermore, the oxygen consumption data were fitted in order to determine the growth rate of the cells on the particles, as described previously [32]. Remarkably, an exponential fit of the data did not correlate as well as a linear fit. Under optimal conditions, one would expect exponential cell growth, but apparently unknown factors are inhibiting the cell growth under these conditions. The data for both fits are shown in Table 2.

Cultures that were seeded at 6 and 12 million cells had a comparable expansion factor, whereas the culture seeded with 1 million cells had a significantly higher growth rate. This could be explained by the fact that cells at lower seeding densities experience less cell–cell contact. It has been described previously that cell–cell contact can stimulate differentiation and inhibit proliferation. Furthermore, we have already reported higher cell proliferation rates when culturing human mesenchymal stem cells on 2D tissue culture flasks at low cell-seeding densities when compared to higher cell-seeding densities [36]. In conclusion, hBMSCs were successfully seeded in different densities and proliferated in a perfusion bioreactor system.

Table 2. Population doubling times, linear expansion factors and their correlation coefficient R^2 after exponential and linear fit of *DO* data of bioreactor runs 1–3

Bioreactor run No.	Seeding density	T_d (d) Exp. fit $y = xe^{ut}$ (R^2)	Expansion factor (d^{-1}) Lin. fit $y = ax + b$ (R^2)
1	1×10^6	57 (0.94)	2.79 (0.98)
2	6×10^6	61 (0.74)	1.86 (0.99)
3	12×10^6	87 (0.94)	1.93 (0.98)

3.1.2. Effect of perfusion rate on hBMSC growth

In runs 5 and 6 (donor 3), cells were cultured at 1 and 4 ml/min, respectively, to evaluate the effect of the perfusion rate (pr) on cell growth. The difference between the ingoing and outgoing oxygen concentration (ΔDO) is depicted in Figure 6.

The ΔDO increases during cultivation for both perfusion rates, but the signal is detected after 7 days when using a perfusion rate of 1 ml/min compared to 15 days for 4 ml/min. Furthermore, a linear reciprocal relationship between the perfusion rate and the ΔDO was observed. The ΔDO reading of culture 5 (pr 1 ml/min) is approximately four times higher than the reading of culture 6 (pr 4 ml/min), as can be seen in Figure 6. After 17 days of cultivation, the ΔDO of culture 5 is about 26%, whereas the ΔDO of culture 6 is about 6%. The difference in ΔDO equals the difference in perfusion rate between the two cultures. This can be explained in terms of the fluid residence time. A decrease in perfusion rate resulted in an increase of the average residence time of a fluid package in the bioreactor, allowing the present cells to consume more oxygen. After 20 days of cultivation, no difference in cell load could be detected between the two perfusion conditions. The particles were largely covered with cells which are depicted in Figure 6A, B. In conclusion, no effect could be observed for the evaluated perfusion rates with respect to the cell load on the particles after cultivation.

3.1.3. Cell metabolism during cultivation

Cells were cultured in a bioreactor system for 40 days in run 9 (donor 5). Medium samples were analysed for glucose, lactate and ammonia concentrations. During cultivation on the glucose consumption increased, as well as lactate and ammonia production (Figure 7). Glucose is used as a carbon and energy source, and lactate and ammonia are waste products of cell metabolism. This indicated cell growth and correlated with an increase in ΔDO during cultivation. A thick layer of living cells was

Copyright © 2009 John Wiley & Sons, Ltd.

DOI: 10.1002/term

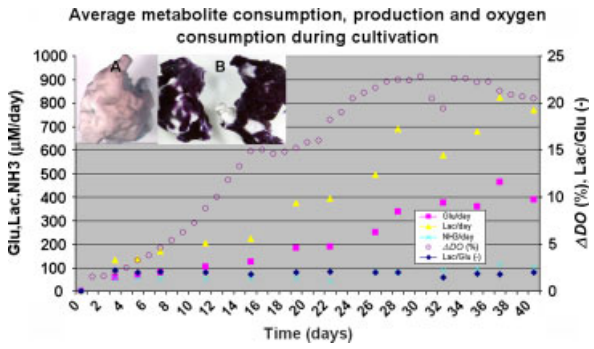

Figure 7. Net dissolved oxygen consumption ($\Delta DO = DO_{in} - DO_{out}$) and metabolite consumption and production during dynamic proliferation of hBMSCs from donor 5 on OsSatura™ BCP particles. (A) The scaffold without cells; (B) MTT stained hBMSCs after 40 days of proliferation

present on the particles even after 40 days of cultivation, as shown by MTT staining in Figure 7.

The molar ratio of lactate produced and the amount of glucose consumed (Qlac : glu) is very close to 2 during the entire cultivation period. The same phenomenon was observed in other runs. This finding suggests that anaerobic glycolysis is the prevalent mechanism for glucose consumption as an energy source [37,38]. This was a surprising finding, since 100% air-saturated medium (containing 20% oxygen) enters the bioreactor. In all cases, we measured dissolved oxygen concentrations at the outlet above 70% of air saturation, which does not represent a hypoxic environment for the cells. The fact that this mechanism is occurring in the presence of oxygen is a phenomenon known as the Warburg effect [39]. At this time, the significance of this effect is not known to us, but future research is going to be conducted in order to unravel the cell metabolism of human BMSCs under different oxygen conditions.

3.2. Characterization of human hybrid constructs produced in a perfusion bioreactor system

3.2.1. In vitro characterization: SEM, collagen type I, ALP expression and quantitative PCR

During visual inspection of the hBMSCs on the BCP particles, it was observed that the hybrid structures became interconnected. For all runs, a dense layer of extracellular matrix was present on and between the particles.

SEM. Characterization of the cell layer and the extra cellular matrix was done using SEM microscopy. Figure 8 shows the development of the cell layer on the BCP surface for bioreactor run 1.

Particles seeded at 1 million cells were visualized during proliferation after 3, 10 and 17 days. Particles seeded at 1 million cells showed few cells after 3 days (Figure 8B) but considerably more after 10 and 17 days (Figure 8C, D). After 17 days the hybrid constructs of bioreactor runs 1 and 3 (donor 1; seeding density 1 and 12 million cells, respectively) showed no difference with respect to the appearance of the cell layer on the particles.

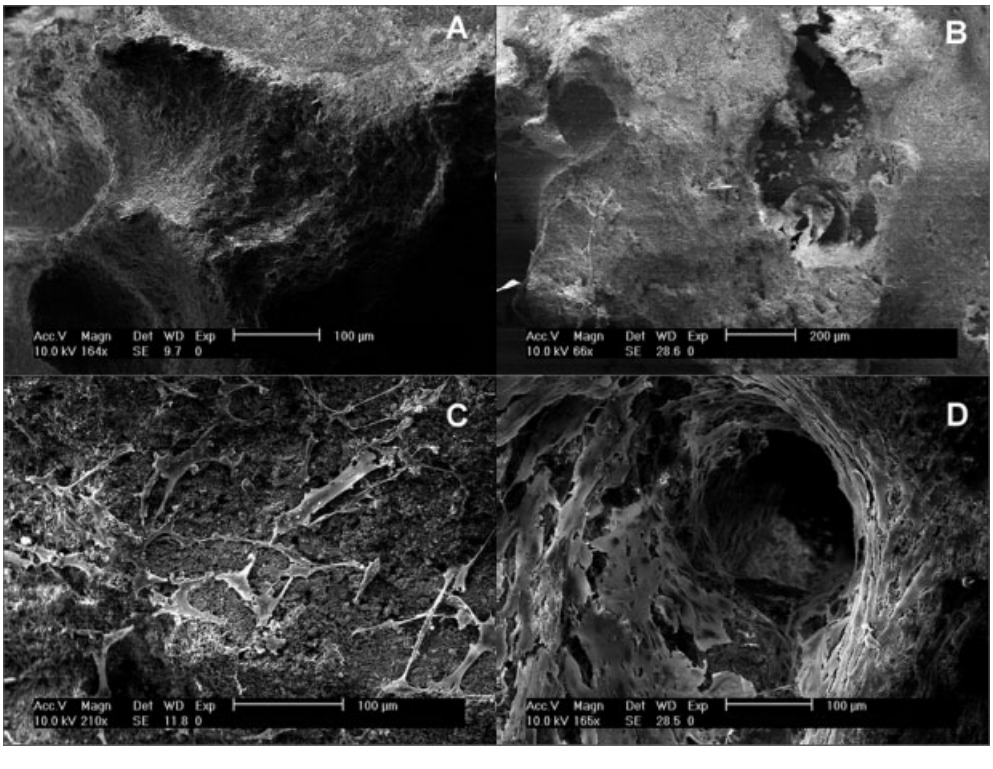

Figure 8. Scanning electron micrograph of hBMSCs cultured on OsSatura™ BCP particles in bioreactor run 1 (seeding density 1×10^6 cells). Scaffold after 0 days (A), after 3 days (B), after 10 days (C) and after 17 days (D)

Copyright © 2009 John Wiley & Sons, Ltd.

DOI: 10.1002/term

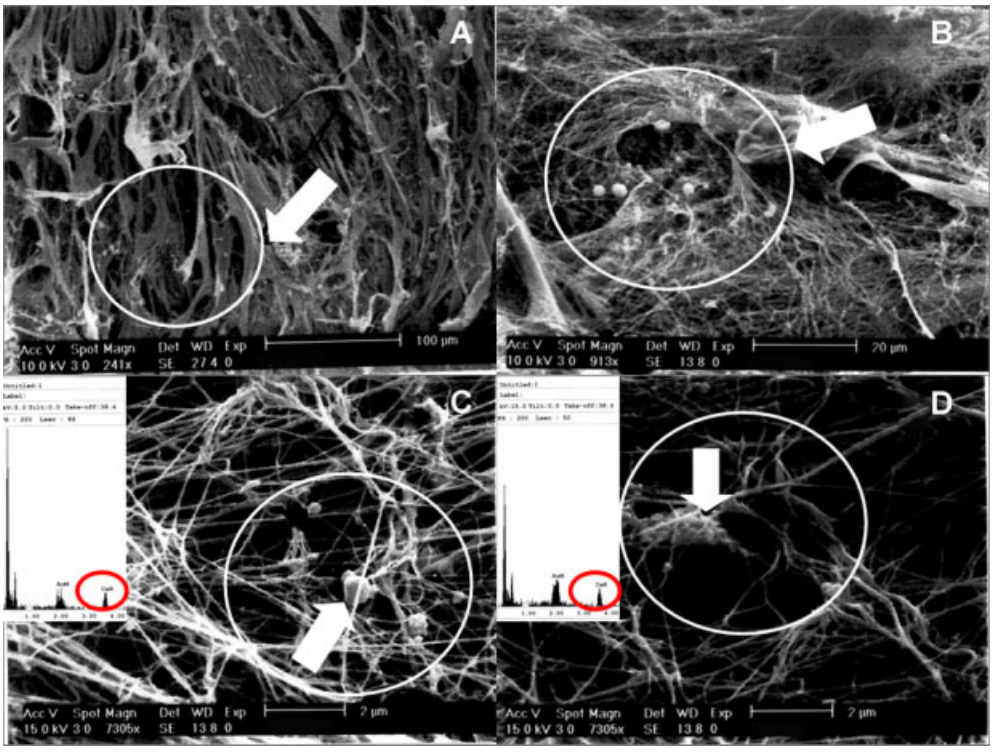

Figure 9. Scanning electron micrograph of hBMSCs on OsSatura™ BCP particles in bioreactor run 4 after 20 days of dynamic proliferation at different magnifications: (A) ×241; (B) ×913; (C, D) ×7305. White arrows and circles depict calcium phosphate nodules as determined by EDX analysis (C, D, red circle)

This was in correspondence with the results of the MB staining shown in Figure 4. On the SEM images, sphere-like structures (±0.5–1 µm) were observed throughout the whole construct. In Figure 9, these nodules are indicated with a white arrow and circle for different magnifications.

EDX analysis showed (red circle) that these nodules consisted of calcium phosphate which is indicative of calcium formation *in vitro*.

Collagen type I and ALP expression. In order to confirm if the hybrid constructs show differentiation towards the osteogenic lineage, the presence of alkaline phosphatase (ALP) and collagen type I was investigated. The results are shown in Figure 10.

Dynamically cultured constructs showed abundant ALP and collagen type I expression (Figure 10A, C, respectively), whereas the controls with cells without primary antibody and controls without cells showed no ALP and collagen type I expression (Figure 10B, D). The presence of extracellular matrix containing calcium phosphate nodules as well as ALP and collagen type I expression proves differentiation towards the osteogenic lineage under *in vitro* conditions, which is in agreement with the previously mentioned studies [28–30].

Quantitative PCR. We observed no significant differences in osteogenic gene expression profiles between static and dynamic conditions in bioreactor runs 11–13 (data not shown). There seemed to be a slightly higher but statistically insignificant ALP expression under dynamic conditions when compared to the statically cultured hybrid constructs. Other osteogenic genes, such as *Cbfa1*, collagen type I, osteocalcin, osteonectin and negative regulator of mineralization *S100A4*, showed no significant difference between static and dynamic conditions. Although we observed a slightly higher induction of BMP2 expression under dynamic conditions, it did not reflect on its target gene expression, such as *Id1, Id2* or *Smad6*.

3.2.2. In vivo characterization: bone formation of hybrid constructs in nude mice

After subcutaneous implantation in nude mice for 6 weeks, the hybrid constructs were explanted, histologically processed and bone formation *in vivo* was assessed. The bone formation for the bioreactor runs is schematically depicted in Table 3.

In seven of eight donors, *in vivo* bone formation was observed in nude mice under both static and dynamic conditions. In Figure 11, the *in vivo* bone formation of dynamically cultured hybrid constructs is shown for donors 1 (11A1-3) and 3 (11B1-2).

The control scaffold without cells is depicted in Figure 11C. *De novo*-formed bone was deposited against the walls of the scaffold material. In many samples, areas with mineralized bone (Figure 11A1–A3 and B1–2, red colour) and osteoid (Figure 11A3 and B1–2, pinkish colour) could be identified. Osteocytes are visible within the bone matrix, and osteoblasts are present in a layer on top of the newly formed bone. Blood vessels (blue

Copyright © 2009 John Wiley & Sons, Ltd.

DOI: 10.1002/term

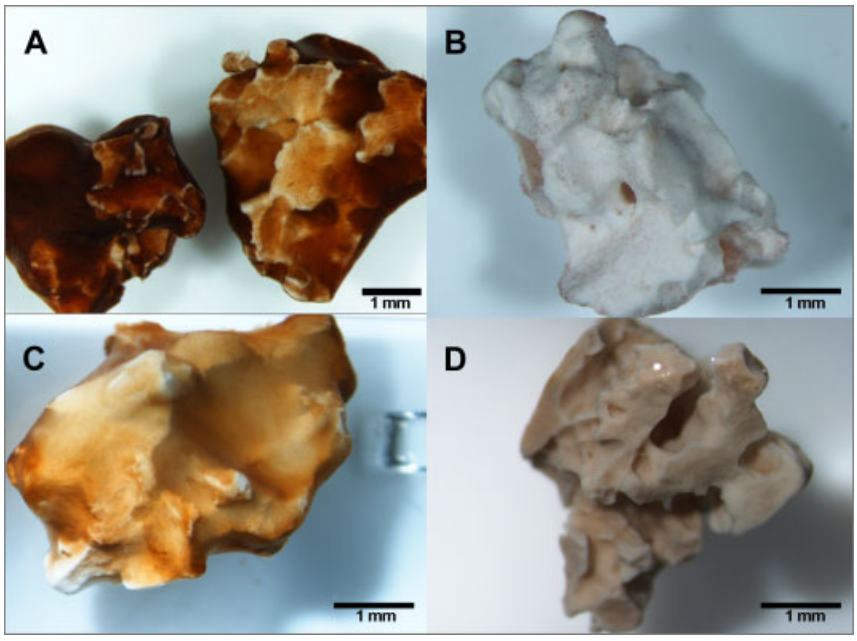

Figure 10. ALP and collagen type I expression (A, C) on hybrid constructs from bioreactor run 9 after 40 days of dynamic proliferation. The controls with cells without primary antibody and controls without cells showed no ALP and collagen type I expression (B, D)

Table 3. Bone formation for all bioreactor runs

Run No.	Donor No.	Passage No.	Amounts of HBMSCs seeded ($\times 10^6$)	*In vivo*: number of mice/number of hybrid constructs implanted	*In vivo* bone formation: static	*In vivo* bone formation: dynamic
1	1	2	1	2/12	+	+
2	1	2	6	2/12	+	+
3	1	2	12	2/12	+	+
4	2	2	12	2/12	−	−
5	3	1	1	2/12	+	+
6	3	1	1	2/12	+	+
7	4	1	1	2/12	+	+
8	4	1	4	2/12	+	+
9	5	5	12	6/36	−	−
10	5	2	12	10/30	+	+
11	6	2	12	10/30	+	+
12	7	2	12	10/30	+	+
13	8	2	12	10/30	+	+

arrow), bone marrow (white arrow) and fat cells (red arrow) were often associated with and in close proximity to newly formed bone.

Most of the statically and dynamically cultivated hybrid constructs showed bone formation *in vivo*. As reported before, an osteogenic phenotype as shown for the hybrid constructs from bioreactor runs 4 and 9 *in vitro* is not predictive for osteogenisis *in vivo* [40]. In seven of eight donors, bone formation was observed in statically as well as dynamically cultured hybrid constructs. Therefore, this effect could not be explained by the difference in cultivation method. *In vivo* bone formation appears to be donor-dependent (run 4 vs. runs 1–3 and 5–9) as well as passage-dependent (run 9 vs. 10, of donor 5), which is in agreement with previous studies [20,41,42]. Varying the seeding density and the perfusion rate during dynamic culturing did not have a distinct effect on the *in vivo* bone formation. In addition, no relationship was found between bone formation and donor age or donor sex. This could be due to the fact that the amount of donors in our study is relatively small ($n = 8$, from which only five were randomly selected) when compared to previous work in which more donors were used and this correlation was seen [43,44]. On the other hand, there are also studies which did not find a correlation between donor age and *in vivo* bone formation [45–47].

In order to assess bone formation quantitatively, we selected four donors (donors 5–8, bioreactor runs 10–13) and cultivated hBMSCs under static and dynamic conditions on ceramic particles. The resulting human hybrid constructs were implanted in a statistically relevant number of nude mice. The *in vivo* bone formation was assessed quantitatively by histomorphometry and is depicted in Figure 12.

Copyright © 2009 John Wiley & Sons, Ltd.

DOI: 10.1002/term

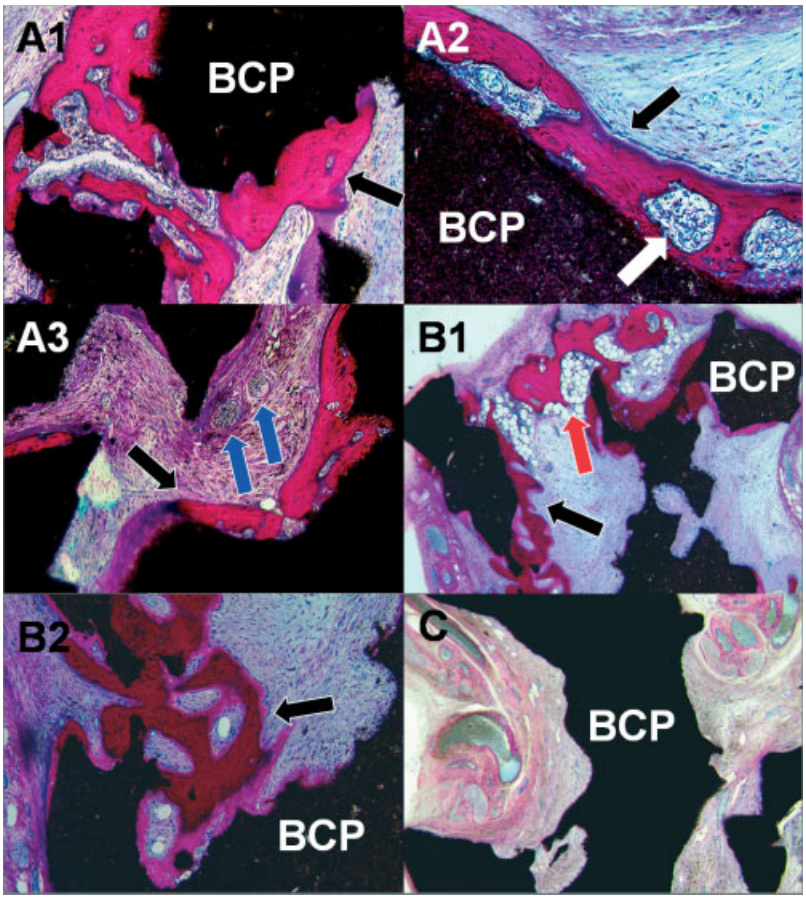

Figure 11. Bone formation by hBMSCs after subcutaneous implantation of dynamically seeded and cultured hybrid constructs from donors 1 (A1–A3) and 3 (B1, B2). New bone (black arrow) is formed on the surface of the OsSatura™ BCP particles (BCP). Bone marrow (white arrow), blood vessel (blue arrow) and fat (red arrow) formation is visible close to newly formed bone tissue

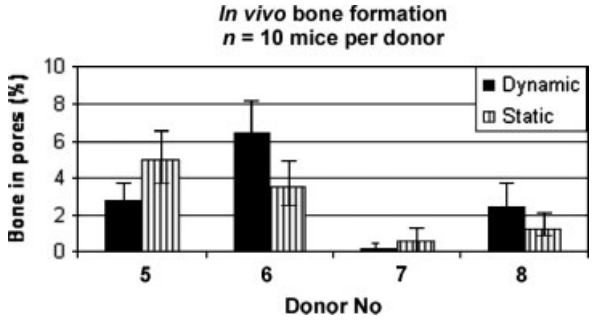

Figure 12. Bone formation by hBMSCs after subcutaneous implantation of dynamically and statically cultured hybrid constructs from donors 5–8. Bone formation was quantitatively assessed by histomorphometry. No significant differences ($p < 0.05$) were observed between static and dynamic conditions for the donors

For these four donors, no statistically significant difference was found between statically and dynamically cultured hybrid constructs ($p < 0.05$). These results differ from the results of Braccini *et al*. [48]. In their studies, implantation of dynamically cultured human hybrid constructs resulted in higher amounts of *in vivo* bone formation in nude mice when compared to statically cultured hybrid constructs. It is possible that the discrepancy between these two studies is caused by the difference in primary isolation of the human BMSCs. In our study, preselection of hBMSCs took place by culturing in 2D tissue culture flasks, whereas Braccini *et al*. directly seeded a ficolled fraction on and in the ceramic scaffold. It has been reported previously that subculturing cells *in vitro* in 2D tissue culture flasks induces loss of multipotency and *in vivo* bone formation [42]. In the future, we will therefore attempt to isolate hBMSCs directly from bone marrow aspirates and seed and culture them on and in ceramic particles in our perfusion system.

Eventually, bone formation in a critical size defect of hybrid constructs produced in bioreactors would result in proof of concept in a large animal model. Previous results showed that viable cells on BCP scaffolds resulted in more bone formation when implanted ectopically in goats when compared to the bare BCP scaffold [49]. However, vascularity in an ectopic acceptor site is much higher when compared to an orthotopic site. Survival of cells in large-sized grafts for orthopaedic reconstruction will be compromised amongst others due to the absence of vascularization during the first week after implantation [50]. Therefore, the ultimate challenge would be to obtain vascularization within the osteogenic construct before implanting it in the acceptor site. This concept is currently being investigated by several groups [51–53].

Copyright © 2009 John Wiley & Sons, Ltd.

DOI: 10.1002/term

4. Conclusions

Dynamic seeding and culturing of human bone marrow stromal cells of different donors on clinically relevant amounts of ceramic scaffold material is feasible by using a semi-automated perfusion bioreactor system. We showed that these cells could be seeded and proliferated on ceramic particles in different seeding densities and at different perfusion rates, until the particles were completely covered. After 20 days a homogeneous and viable cell layer could be observed based on MB and MTT staining, which corresponded with online measurements of oxygen consumption during the cultivation period. The hybrid structures became interconnected and a dense layer of extracellular matrix was present as visualized by environmental scanning electron microscopy (SEM). SEM images showed, within the extracellular matrix, sphere-like structures that were identified as calcium phosphate nodules by energy dispersive X-ray analysis (EDX). Furthermore, these cells show differentiation towards the osteogenic lineage, as was shown by collagen type I production and ALP expression. We observed no significant differences in osteogenic gene expression profiles, such as *ALP, BMP2, Id1, Id2, Smad6*, collagen type I, osteocalcin, osteonectin and *S100A4*, between static and dynamic conditions. Subcutaneous implantation of hybrid constructs in nude mice consisting of OsSatura™ BCP particles and human BMSCs cultivated under dynamic and static conditions resulted in *de novo* bone formation in a donor-dependent way. In seven of eight donors that showed bone formation, dynamically cultured hybrid constructs showed the same amount of bone as the statically cultured hybrid constructs. When *in vivo* bone formation was quantitatively assessed by histomorphometry for four donors, no statistically significant difference was found between statically and dynamically cultured hybrid constructs.

Acknowledgements

The authors thank Helma Peters and Inge Hofland for excellent technical support, Sanne Both for the implantation studies in nude mice and Ramakrishnaiah Siddappa for RNA isolation and qPCR analysis. We would also like to thank Huipin Yuan for providing us with OsSatura™ BCP scaffold material and Kruba Shankar Sivasubramanyam for microCT analysis of the scaffold bed in the bioreactor. We thank Applikon Dependable Instruments B.V. for the co-development and production of the bioreactor system.

References

1. Bianco P, Gehron RP. 2000; Marrow stromal stem cells. *J Clin Invest* **105**(12): 1663–1668.
2. Colter DC, Sekiya I, Prockop DJ. 2001; Identification of a subpopulation of rapidly self-renewing and multipotential adult stem cells in colonies of human marrow stromal cells. *Proc Natl Acad Sci USA* **98**(14): 7841–7845.
3. Jiang Y, Jahagirdar BN, Reinhardt RL, *et al*. 2002; Pluripotency of mesenchymal stem cells derived from adult marrow. *Nature* **418**(6893): 41–49.
4. Horwitz EM, Prockop DJ, Fitzpatrick LA, *et al*. 1999; Transplantability and therapeutic effects of bone marrow-derived mesenchymal cells in children with osteogenesis imperfecta. *Nat Med* **5**(3): 309–313.
5. Le Blanc K, Rasmusson I, Sundberg B, *et al*. 2004; Treatment of severe acute graft-versus-host disease with third party haploidentical mesenchymal stem cells. *Lancet* **363**(9419): 1439–1441.
6. Javazon EH, Beggs KJ, Flake AW. 2004; Mesenchymal stem cells: paradoxes of passaging. *Exp Hematol* **32**(5): 414–425.
7. Friedenstein AJ, Latzinik NW, Grosheva AG, *et al*. 1982; Marrow microenvironment transfer by hetrotopic transplantation of freshly isolated and cultured cells in porous sponges. *Exp Hematol* **10**(2): 217–227.
8. Allay JA, Dennis JE, Haynesworth SE, *et al*. 1997; LacZ and interleukin-3 expression *in vivo* after retroviral transduction of marrow-derived human osteogenic mesenchymal progenitors. *Hum Gene Ther* **8**(12): 1417–1427.
9. Bruder SP, Kurth AA, Shea M, *et al*. 1998; Bone regeneration by implantation of purified, culture expanded human mesenchymal stem cells. *J Orthop Res* **16**(2): 155–162.
10. Cui Q, Ming Xiao Z, Balian G, *et al*. 2001; Comparison of lumbar spine fusion using mixed and cloned marrow cells. *Spine* **26**(21): 2305–2310.
11. Krebsbach PH, Mankani MH, Satomura K, *et al*. 1998; repair of craniotomy defects using bone marrow stromal cells. *Transplantation* **66**(10): 1272–1278.
12. van Gaalen SM, Dhert WJ, van den Muysenberg A, *et al*. 2004; Bone tissue engineering for spine fusion: an experimental study on ectopic and orthopic implants in rats. *Tissue Eng* **10**(1–2): 231–239.
13. Meijer GJ, de Bruijn JD, Koole R, *et al*. 2007; Cell-based bone tissue engineering. *PLoS Med* **4**(2): e9.
14. Mendes SC, van den Brink I, de Bruijn JD, *et al*. 1998; *In vivo* bone formation by human bone marrow cells: effect of osteogenic culture supplements and cell densities. *J Mater Sci Mater Med* **9**(12): 855–858.
15. de Bruijn JD, van den Brink I, Bovell YP, *et al*. 1998; Tissue engineering of goat bone: osteogenic potential of goat bone marrow cells. *Bioceramics* **11**: 497–500.
16. Aubin JE. 1998; Bone stem cells. *J Cell Biochem Suppl* **30–31**: 73–82.
17. de Bruijn JD, van Blitterswijk CA. 1998; New developments in implant coatings: biomimetics and tissue engineering. In *Biomaterials in Surgery*, G. Walenkamp (ed.). Georg Thieme Verlag: Stuttgart; 77–82.
18. Martin I, Wendt D, Heberer M. 2004; The role of bioreactors in tissue engineering. *Trends Biotechnol* **22**(2): 80–86.
19. Banfi A, Muraglia A, Dozin B, *et al*. 2000; Proliferation kinetics and differentiation potential of *ex vivo* expanded human bone marrow stromal cells: implications for their use in cell therapy. *Exp Hematol* **28**(6): 707–715.
20. Mendes SC, Tibbe JM, Veenhof M, *et al*. 2002; Bone tissue-engineered implants using human bone marrow stromal cells: effect of culture conditions and donor age. *Tissue Eng* **8**(6): 911–920.
21. Abbott A. 2003; Cell culture: biology's new dimension. *Nature* **424**(6951): 870–872.
22. Steffen T, Tsantrizos A, Fruth I, *et al*. 2000; Cages: designs and concepts. *Eur Spine J* **9**(suppl 1): S89–94.
23. de Bruijn JD, van den Brink I, Bovell YP, *et al*. 1998; Tissue engineering of goat bone: osteogenic potential of goat bone marrow cells. *Bioceramics* **11**: 497–500.
24. Ishaug-Riley SL, Crane-Kruger GM, Yaszemski MJ, *et al*. 1998; Three dimensional culture of rat calvarial osteoblasts in porous biodegradable polymers. *Biomaterials* **19**(15): 1405–1412.
25. Holy CE, Shoichet MS, Davies JE. 2000; Engineering three-dimensional bone tissue *in vitro* using biodegradable scaffolds: investigating cell density and culture period. *J Biomed Mater Res* **51**(3): 376–382.
26. Bancroft GN, Sikavitsas VI, Mikos AG. 2003; Design of a flow perfusion bioreactor system for bone tissue engineering applications. *Tissue Eng* **9**(3): 549–554.

Copyright © 2009 John Wiley & Sons, Ltd.

27. Cartmell SH, Porter BD, Garcia AJ, *et al*. 2003; Guldberg RE. Effects of medium perfusion rate on cell-seeded three-dimensional bone constructs *in vitro*. *Tissue Eng* **9**(6): 1197–1203.
28. Sikavitsas VI, Bancroft GN, Holtorf HL, *et al*. 2003; Mineralized matrix deposition by marrow stromal osteoblasts in 3D perfusion culture increases with increasing fluid shear forces. *Proc Natl Acad Sci USA* **100**(25): 14683–14688.
29. Bancroft GN, Sikavitsas VI, van den Dolder J, *et al*. 2002; Fluid flow increases mineralized matrix deposition in 3D perfusion culture of marrow stromal osteoblasts in a dose-dependent manner. *Proc Natl Acad Sci USA* **99**(20): 12600–12605.
30. Goldstein AS, Juarez TM, Helmke CD, *et al*. 2001; Effect of convection on osteoblastic cell growth and function in biodegradable polymer foam scaffolds. *Biomaterials* **22**(11): 1279–1288.
31. Wang Y, Uemura T, Dong J, *et al*. 2003; Application of perfusion culture system improves *in vitro* and *in vivo* osteogenesis of bone marrow derived osteoblastic cells in porous ceramic materials. *Tissue Eng* **9**(6): 1205–1214.
32. Janssen FW, Oostra J, van Oorschot A, *et al*. 2006; A perfusion bioreactor system capable of producing clinically relevant volumes of tissue engineered bone: *in vivo* bone formation showing proof of concept. *Biomaterials* **27**(3): 315–323.
33. Janssen FW, Hofland I, van Oorschot A, *et al*. 2006; Online measurement of oxygen consumption by bone marrow stromal cells in a combined cell-seeding and proliferation bioreactor. *J Biomed Mater Res A* **79**(2): 338–348.
34. Yuan H, van den Doel M, Li S, *et al*. 2002; A comparison of the osteoinductive potential of two calcium phosphate ceramics implanted intramuscularly in goats. *J Mater Sci Mater Med* **13**(12): 1271–1275.
35. Livak KJ, Schmittgen TD. 2001; Analysis of relative gene expression data using real-time quantitative PCR and the $2(-\Delta\Delta C^T)$ method. *Methods* **25**: 402–408.
36. Both SK, van der Muijsenberg AJ, van Blitterswijk CA, *et al*. 2007; A rapid and efficient method for expansion of human mesenchymal stem cells. *Tissue Eng* **13**(1): 3–9.
37. Newsholme P, Newsholme EA. 1989; Rates of utilization of glucose, glutamine and oleate and formation of end-products by mouse peritoneal macrophages in culture. *Biochem J* **261**(1): 211–218.
38. Ozturk SS, Palsson BO. 1991; Growth, metabolic, and antibody kinetics of hybridoma cell culture: 2. Effect of serum concentration, dissolved oxygen concentration, and medium pH in a batch reactor. *Biotechnol Prog* **7**(6): 481–494.
39. Bartrons R, Caro J. 2007; Hypoxia, glucose metabolism and the Warburg's effect. *J Bioenerg Biomembr* **39**(3): 223–229.
40. Habibovic P, Woodfield T, de Groot K, *et al*. 2006; Predictive value of *in vitro* and *in vivo* assays in bone and cartilage repair – what do they really tell us about the clinical performance? *Adv Exp Med Biol* **585**: 327–360.
41. Siddappa R, Licht R, Van Blitterswijk C, *et al*. 2007; Donor variation and loss of multipotency during *in vitro* expansion of human mesenchymal stem cells for bone tissue engineering. *J Orthop Res* **25**(8): 1029–1041.
42. Siddappa R, Fernandez H, Liu J, *et al*. 2007; The response of human mesenchymal stem cells to osteogenic signals and its impact on bone tissue engineering. *Curr Stem Cell Res Ther* **2**(3): 209–220.
43. Bab I, Passi-Even L, Gazit D, *et al*. 1988; Osteogenesis in *in vivo* diffusion chamber cultures of human marrow cells. *Bone Miner* **4**(4): 373–386.
44. Mendes SC, Tibbe JM, Veenhof M, *et al*. 2002; Bone tissue-engineered implants using human bone marrow stromal cells: effect of culture conditions and donor age. *Tissue Eng* **8**(6): 911–920.
45. Stenderup K, Rosada C, Justesen J, *et al*. 2004; Aged human bone marrow stromal cells maintaining bone forming capacity *in vivo* evaluated using an improved method of visualization. *Biogerontology* **5**(2): 107–118.
46. Stenderup K, Justesen J, Clausen C, *et al*. 2003; Aging is associated with decreased maximal life span and accelerated senescence of bone marrow stromal cells. *Bone* **33**(6): 919–926.
47. De Bari C, Dell'Accio F, Vanlauwe J, *et al*. 2006; Mesenchymal multipotency of adult human periosteal cells demonstrated by single-cell lineage analysis. *Arthritis Rheum* **54**(4): 1209–1221.
48. Braccini A, Wendt D, Jaquiery C, *et al*. 2005; Three-dimensional perfusion culture of human bone marrow cells and generation of osteoinductive grafts. *Stem Cells* **23**(8): 1066–1072.
49. Kruyt MC, Dhert WJ, Oner C, *et al*. 2004; Optimization of bone tissue engineering in goats: a peroperative seeding method using cryopreserved cells and localized bone formation in calcium phosphate scaffolds. *Transplantation* **77**: 504–509.
50. Decker S, Muller-Farber J, Decker B. 1979; New bone formation in an autologous spongy graft: an experimental morphological study. *Z Plast Chir* **3**: 159–175.
51. Young PP, Vaughan DE, Hatzopoulos AK. 2007; Biologic properties of endothelial progenitor cells and their potential for cell therapy. *Prog Cardiovasc Dis* **49**(6): 421–429.
52. Scherberich A, Galli R, Jaquiery C, *et al*. 2007; Three-dimensional perfusion culture of human adipose tissue-derived endothelial and osteoblastic progenitors generates osteogenic constructs with intrinsic vascularization capacity. *Stem Cells* **25**(7): 1823–1829.
53. Rouwkema J, Westerweel PE, de Boer J, *et al*. 2009; The use of endothelial progenitor cells for prevascularized bone tissue engineering. *Tissue Eng* (in press).

Copyright © 2009 John Wiley & Sons, Ltd.

DOI: 10.1002/term